



HAL
open science

Unravelling caramelization and Maillard reactions in glucose and glucose + leucine model cakes: Formation and degradation kinetics of precursors, α -dicarbonyl intermediates and furanic compounds during baking

J. Lee, Stéphanie Roux, E. Le Roux, S. Keller, Barbara Rega, C. Bonazzi

► To cite this version:

J. Lee, Stéphanie Roux, E. Le Roux, S. Keller, Barbara Rega, et al.. Unravelling caramelization and Maillard reactions in glucose and glucose + leucine model cakes: Formation and degradation kinetics of precursors, α -dicarbonyl intermediates and furanic compounds during baking. *Food Chemistry*, 2022, 376, pp.131917. 10.1016/j.foodchem.2021.131917. hal-03819621

HAL Id: hal-03819621

<https://agroparistech.hal.science/hal-03819621>

Submitted on 18 Oct 2022

HAL is a multi-disciplinary open access archive for the deposit and dissemination of scientific research documents, whether they are published or not. The documents may come from teaching and research institutions in France or abroad, or from public or private research centers.

L'archive ouverte pluridisciplinaire **HAL**, est destinée au dépôt et à la diffusion de documents scientifiques de niveau recherche, publiés ou non, émanant des établissements d'enseignement et de recherche français ou étrangers, des laboratoires publics ou privés.



Distributed under a Creative Commons Attribution - NonCommercial 4.0 International License

Unravelling caramelization and Maillard reactions in glucose and glucose+leucine model cakes: formation and degradation kinetics of precursors, α -dicarbonyl intermediates and furanic compounds during baking.

Lee, J., Roux, S.* , Le Roux, E., Keller, S., Rega, B., Bonazzi, C.

Université Paris-Saclay, INRAE, AgroParisTech, UMR SayFood, 91300, Massy, France

Food Chemistry 376 (2022) 13197

<https://doi.org/10.1016/j.foodchem.2021.131917>

Highlights:

- Caramelization & Maillard paths were clarified for glucose and leucine as precursors
- 12 markers were measured quantitatively in a model cake versus baking time
- Kinetic data consolidated the reaction scheme
- The impact of temperature, convection and formula on the reactions was studied
- The importance of isomerization of glucose to fructose was highlighted

Chemical compounds studied in this article:

Glucose (PubChem CID: 107526)

Fructose (PubChem CID: 2723872)

Leucine (PubChem CID: 6106)

Glyoxal (PubChem CID: 7860, IUPAC name: oxaldehyde)

Methylglyoxal (PubChem CID: 880, IUPAC name: 2-oxopropanal)

Diacetyl (PubChem CID: 650, IUPAC name: Butane-2,3-dione)

Glucosone (PubChem CID: 159630, IUPAC name: (4*S*,5*R*)-4,5,6-trihydroxy-2-oxohexanal)

1-deoxyglucosone (PubChem CID: 11228966, IUPAC name: (4*R*,5*R*)-4,5,6-trihydroxyhexane-2,3-dione)

3-deoxyglucosone (PubChem CID: 114839, IUPAC name: (4*S*,5*R*)-4,5,6-trihydroxy-2-oxohexanal)

3,4-dideoxyglucosone (PubChem CID: 132520491, IUPAC name: (5*R*)-5,6-dihydroxy-2-oxohexanal)

Furfural (PubChem CID: 7362, IUPAC name: furan-2-carbaldehyde)

5-hydroxymethylfurfural (PubChem CID: 237332, IUPAC name: 5-(hydroxymethyl)furan-2-carbaldehyde)

* Corresponding author: Dr Stéphanie Roux, Paris-Saclay Food and Bioproduct Engineering Research Unit, Campus Agro Paris-Saclay, 22 Place de l'Agronomie, 91120 Palaiseau, France; +33 189101170; stephanie.roux@agroparistech.fr
Other authors' e-mail addresses: jeehyun.lee@agrocampus-ouest.fr; even.leroux@agroparistech.fr; severine.keller@agroparistech.fr; barbara.rega@agroparistech.fr; catherine.bonazzi@inrae.fr

Abstract:

Understanding the mechanisms leading to the multitude of newly-formed compounds generated during the thermal processing of food is important for the reasoned construction of quality. Thanks to a solid food model with a structure and technological history comparable to that of a real sponge cake and containing only known amounts of precursors (glucose with or without leucine), an adapted reaction scheme unravelling Maillard and caramelization reactions was built and then compared to experimental kinetic data measured on numerous reaction markers (precursors, α -dicarbonyl intermediates and furanic compounds). For caramelization, this study showed that glucose mainly formed 1,2-enediol and then fructose rather than glucosone and glyoxal. 5-hydroxymethylfurfural started to form when there were sufficient quantities of fructose, and 3,4-dideoxyglucosone was not generated until after this step. Furfural was mainly formed *via* 3-deoxyglucosone. The involvement of leucine tended to accelerate the breakdown of sugars as more degradation pathways (*via* enaminals) were added.

Keywords: Deoxyglucosone, furfural, 5-hydroxymethylfurfural, reaction pathways, heat transfer

1 Introduction

The Maillard reaction has not yet been fully elucidated, although many scientists have exploited and improved the comprehensive reaction scheme proposed by Hodge (1953). In a complex food, the Maillard reaction almost always interacts with other pathways such as caramelization and lipid oxidation (Hidalgo et al., 1999).

The majority of words related to browning reactions and/or bakery products can be classified according to two themes: structure complexity and precursor diversity and complexity. Because of the complexity of the reaction network formed by both the Maillard reaction and caramelization, many authors have used liquid and semi-liquid model systems to focus on specific pathways by using selected precursors (Gökmen et al., 2012; Jusino et al., 1997; Rainer Cremer & Eichner, 2000). The use of such liquid systems is appropriate to discriminate specific reaction pathways, but transposition to solid foods has limitations because the reduced mobility of the precursors, the influence of the porous structure, and the heat and mass gradients induced by heat treatment are not considered.

More or less complex solid systems such as products to those with honeycomb solids (bread, cakes) have been used relevantly to study the impact of ingredients and processes on the generation of quality-related compounds (Ait Ameer et al., 2008; Cepeda-Vázquez et al., 2018) or for mitigation strategies with respect to health-related compounds (Gökmen et al., 2007). However, precursors and intermediates were rarely measured and are difficult to control.

As a relatively novel approach, multi-response kinetic modelling has been of considerable assistance to better understand reaction pathways in food products, as it is a robust tool to clarify the rate-determining steps in complex reactions and thus to understand the mechanisms (De Vleeschouwer et al., 2009; Martins et al., 2000). This approach has been applied successfully to monitoring and modeling the Maillard reaction in different reaction media (Carline M. J. Brands & van Boekel, 2003; Göncüoğlu Taş & Gökmen, 2017; Kocadağlı & Gökmen, 2016; Martins & van Boekel, 2003; Nguyen et al., 2016; Srivastava et al., 2018), but it requires accurate quantitative measurements of reaction markers and appropriate reaction media to study kinetics in a controlled environment in terms of the quantity and nature of reaction precursors.

Establishing the link between composition, reactivity and quality determinants is therefore not a simple task because of the interdependency of physical and chemical parameters and the complexity of real food ingredients. Studying complex transformations in a food matrix under strictly controlled physical, structural and chemical conditions is therefore paramount value when trying to verify the hypotheses based on many decades of results obtained in simple model systems (far from real foods) or in real products (albeit with a limited understanding of specific reaction pathways).

In previous papers (Lee et al., 2020; Srivastava et al., 2018), the use of a model cake containing glucose with or without leucine has been shown to be highly relevant to follow the reactivity of a solid product. This model cake imitates sponge cake in terms of its alveolar structure and manufacturing method (using same operations of mixing, foaming and baking). Leucine, one of the 8 essential amino acids, was chosen since it is the precursor of 3-methylbutanal, a key aroma compound of cereal products (Zehentbauer & Grosch, 1998).

The aim of the present study was to discuss kinetic concentration data for 12 markers (precursors, intermediates and furanic compounds) obtained during the baking of model cakes containing glucose with or without leucine as reactants. Thermal reactivity was induced under strictly controlled processing conditions at three temperatures and two levels of convection which were monitored thorough baking.

2 Materials and Methods

2.1 Ingredients and reagents

Model sponge cakes were prepared from water purified through an Integral 3 (Millipore, Bedford, MA, USA) water system, native corn starch (12.4% w/w water, Cargill, Wayzata, MN, USA), and food grade methylcellulose (MC, type SGA7C) and hydroxypropyl methyl cellulose (HPMC, type K250M) (Dow Chemicals, Midland, MI, USA). D-(+)-Glucose (Glu) and L-Leucine (Leu) ($\geq 99\%$, Food Grade), used as precursors, were purchased from Roquette Frères (Lestrem, France) and Sigma-Aldrich (St. Louis, MO, USA), respectively.

D-(+)-Glucose ($\geq 99.5\%$), D-(-)-Fructose (Fru) ($\geq 99\%$), furfural (F) ($\geq 99\%$), 5-hydroxymethylfurfural (5-HMF) ($\geq 99\%$), ammonia solution at $\sim 25\%$ (LC-MS grade), quinoxaline ($> 99\%$), methylquinoxaline ($> 97\%$), dimethylquinoxaline ($\geq 99\%$), o-phenylenediamine (o-PDA) ($> 99\%$), diethylenetriaminepentaacetic acid (DETAPAC) ($> 99\%$), and acetonitrile ($\geq 99.9\%$, HPLC grade) were all purchased from Sigma-Aldrich (St. Louis, MO, USA). Quinoxaline-5,6,7,8-d4 (internal standard) was obtained from Cluzeau Info Labo (Saint-Foy-La-Grande, France). Water, acetonitrile, water + 0.1% HCOOH (v/v), acetonitrile + 0.1% HCOOH (v/v), methanol, formic acid ($> 99\%$), all LC-MS grade, sodium phosphate monobasic dihydrate ($> 99\%$) and sodium phosphate dibasic dihydrate ($> 99\%$), Carrez Reagent I and II, formaldehyde 30%, and 0.005 N NaOH solution were all purchased from Carlo Erba Reagents (Val-De-Reuil, France).

2.2 Preparation, baking and sampling of model cakes

2.2.1 Batter preparation and baking

The model cakes were prepared according to the procedure described in Lee et al., (2020) using a hydrocolloid solution of HPMC and MC foamed with corn starch and enriched prior to baking with glucose (*G*) or glucose and leucine (*G+L*), as the only precursors. Twenty grams of batter were poured into disposable cylindrical aluminum molds (diameter = 6.6 cm, mold height = 4 cm, cake height = 1.3 cm), and 14 (at 140°C) or 16 (at 170°C or 200°C) cakes were baked at the same time in an instrumented pilot oven with precise and uniform control of temperature (Bongard, Wolfisheim, France) (Fehaili et al., 2010). Baking experiments for both *G* and *G+L* model cakes were conducted at three temperatures: 140°C, 170°C and 200°C, and two fan frequencies: 25 and 50 Hz. The baking trials at 170°C were performed in triplicate.

2.2.2 Sampling of cakes during baking and preparation of samples for analysis

Model cakes were sampled from the oven at different times during baking: 0, 6, 12, 24, 37, 56, 75 and 90 min. For the baking experiments at 140°C, two additional times (105 and 120 min) were added for *G* model and for *G+L* model, 90 min was replaced by 95 min and a sampling at 120 min was also added. Such long durations (90-120 mins) were selected in order to push the degradation of the substrates and to reveal the behaviors of the intermediates as completely as possible.

Immediately after sampling, the model cakes were sealed in previously tared aluminum bags (Multivac, Lagny-sur-Marrie, France) and plunged into a water/ethanol bath at -8°C for a minimum of 15 min in order to halt any further reactions. The samples were then stored at -20°C for 24 to 48 hours before being frozen at -80°C for 24 hours and freeze-dried in a LCS laboratory device with an ice condenser temperature of -85°C (Martin Christ, Osterode am Harz, Germany). Finally, the samples were ground for 1 min using an electric chopper (Moulinex, Ecully, France), divided into eight aliquots and stored frozen at -20°C until analysis.

2.2.3 Determination of moisture content

The dry matter content of freeze-dried aliquots was determined by desiccation for 24 h at 105°C in a ventilated oven. The moisture content of the cakes was calculated from the difference in mass between the initial dough (precision 10^{-2} g) and the sampled cake (precision 10^{-4} g).

2.3 Temperature measurements and data acquisition system

All temperatures were measured using 1 mm diameter J-type thermocouples (individually calibrated using a calibration oven (Wika, Klingenberg am Main, Germany) and a certified probe (Testo, Forbach, France) automatically recorded every 2 s by a data logger driven by Labview (National instruments, Austin, TX, USA). Three thermocouples were inserted horizontally at different heights in a model cake. The first one measured the temperature on the central axis and at the interface between the cake and the mold (bottom); the second was also on the central axis but at half height of the cake (center); and the third was at the periphery of the cake (across the cake until 0.1 cm from the opposite side) and at the interface between the cake and the air (surface).

2.4 Determination of the degree of browning

Water-soluble brown pigments were extracted at 20°C (0.8 g of freeze-dried sample/25 g Ultrapure water). After homogenization with a vortex for 30 s/3000 rpm, the extract was filtered using filter papers (particle retention = 8 µm, Whatman, Maidstone, UK). The absorbance of the supernatant was measured using a UV-vis spectrometer (Secomam S250, Aqualabo Analyse, France) at 420 nm. Appropriate dilutions were performed in order to obtain an absorbance value lower than 1. The degree of browning was calculated using the dry matter content and the dilution ratio of the sample.

2.5 Analysis of glucose and fructose

2.5.1 Extraction and sample preparation

Monosaccharides were extracted at 20°C (0.4 g of freeze-dried sample/20 g Ultrapure water). The extract was homogenized with a vortex for 30 s/3000 rpm and centrifuged at 5000g for 15 min. 10 g of supernatant were mixed with 0.5 mL Carrez I and 0.5 mL Carrez II reagents. The solution was homogenized with a vortex for 30 s/3000 rpm and then centrifuged at 10000g for 2 min. The supernatant was filtered through a 0.2 µm hydrophilic nylon membrane (Thermo Scientific, Waltham, MA, USA) and placed in a vial.

2.5.2 Separation, identification and quantification by UHPLC-CAD

Glucose and fructose were separated and detected by UHPLC using a Dionex U3000 system (Thermo Fisher, Waltham, MA, USA) equipped with a trinary solvent manager RS pump, a refrigerated RS autosampler at 10°C

and a RS Column compartment oven heated at 35°C, coupled to a Corona™ Veo™ RS Charged Aerosol Detector (CAD). The stationary phase was a 100 x 2.1 mm Acquity BEH Amide column containing 1.7 µm diameter porous spherical particles (Waters, Milford, MA, USA).

The mobile phase was composed of Water (A) and Acetonitrile (B), both alkalized with 10 mM NH₄OH, flowing at 0.26 mL.min⁻¹. The gradient started at 20% A, was maintained for 4 min and then reached 50% A in 3 min. This composition was kept for 3 min to rinse the system before returning back to 20% A in 0.5 min and finally equilibrating for 8.5 min, the total run duration being 19 min. The data were processed using Chromeleon® v7.2 software. The injection volume was 2 µL.

Calibration with an external standard method was used for quantification. The response range was evaluated for concentrations ranging from 0.01 to 3 g.L⁻¹ at 4-6 points. The response was quadratic with the peak area on the ordinates and the concentration on the abscissa, without forcing the zero-crossing. The *LOD* and *LOQ* values for glucose were equal to 7.803 and 26.01 mg.L⁻¹, respectively, while for fructose they were equal to 9.339 and 31.13 mg.L⁻¹, respectively.

2.6 Analysis of free NH₂

Titration against 0.005 N NaOH using a 809 Titrand auto-titrator (Metrohm, Herisau, Switzerland) was performed to measure the concentrations of the free amino group from leucine according to the procedure described in Lee et al., (2020). The concentration of free amino group was expressed in moles of NH₂ per gram of dry matter.

The linearity range of this method was evaluated at six concentration points within the range 0.0039 - 0.0382 mmol.g⁻¹. The *LOD* and *LOQ* values were equal to 0.761 and 2.536 µmol.g⁻¹, respectively.

2.7 Analysis of α-dicarbonyl intermediates

2.7.1 Extraction and sample preparation for α-dicarbonyl analysis

α-dicarbonyl compounds were extracted at 20°C (0.4 g of freeze-dried sample/20 g Ultrapure water). After homogenization with a vortex for 30 s/3000 rpm, the extract was centrifuged at 5000g for 15 min, and then 5 mL of supernatant were mixed with 5 mL of acetonitrile, homogenized with a vortex for 30 s/3000 rpm, and centrifuged at 7000g for 3 min in order to precipitate colloidal polymers.

The derivatization of 900 µL of the recovered supernatant was performed by adding 150 µL phosphate buffer pH 7.0 (100 mmol.L⁻¹) and 150 µL o-PDA at 0.2% in DETAPAC (10 mmol.L⁻¹) and heating the mixture at 60°C for 30 min. It was then cooled in ambient air for 1 min, and 100 µL of quinoxaline-5,6,7,8-d4 (10 mg.L⁻¹) was added as an internal standard. The mixture was then homogenized, filtered through 0.2 µm hydrophilic nylon membrane (Thermo Fisher Scientific, Waltham, MA, USA), and placed in a vial for analysis.

2.7.2 Separation, identification and quantification by UHPLC-MS-QToF

The quinoxaline derivatives of glucosone, 1-deoxyglucosone, 3-deoxyglucosone, 3,4-dideoxyglucosone, glyoxal, methylglyoxal and diacetyl were separated and detected by UHPLC using an Acquity H-Class apparatus (Waters, Milford, MA, USA) composed of a quaternary solvent manager pump (QSM), a refrigerated sample manager at 10°C Flow Trough Needle (SM-FTN), a column oven heated at 30°C, and a high resolution mass spectrometer (MS) with a Xevo® G2-XS QToF Quadrupole Time-of-Flight analyzer (QToF), equipped with an Electrospray Ionization Source (ESI).

The stationary phase was a Purospher® STAR RP-18e column (150 x 4.6 mm, 5 µm) (Merck, Darmstadt, Germany). The injection volume was 1 µL.

Elution was carried out using a 0.3 mL.min⁻¹ flow rate with water (LC/MS Grade, acidified with 1% formic acid)/methanol (LC/MS Grade, acidified with 1% formic acid) with the following gradient: from 70% to 40% water in 10 min, then back to 70% in 2 min, and finally equilibrating the system for 3 min, the total run duration being 15 min.

All the MS analyses were performed in positive polarity using the resolution mode for a scan time of 0.5 s, with a mass range between 50 m/z and 600 m/z acquired in centroid. The QToF analyzer was internally calibrated with a continuous flow at 5 µL.min⁻¹ of Leucine Enkephalin at 1 mg.L⁻¹ for 3 scans every 20 s for 0.2 s. The ESI+ parameters used for the analyses were: capillary voltage of 0.5 kV, sampling cone of 40 V, a source offset of 80 V, a cone gas flow of 50 L.h⁻¹, and a desolvation gas flow of 1000 L.h⁻¹. The source and the desolvation gas were heated at 120°C and 500°C, respectively.

Chromatographic peak areas for each compound were calculated by extracting the chromatograms at the exact masses of the specific ions using MassLynx (Milford, MA, USA) (Table 1).

Table 1. Derivative forms of α-dicarbonyl compounds associated with their retention times and selected quantifier ions

Compound	Retention time (min)	Selected ion (m/z)
Glucosone (GCO) derivative	3.52	235.1077
1-Deoxyglucosone (1-D) derivative	4.10	217.0971
3-Deoxyglucosone (3-D) derivative	4.48	217.0971
3,4-Dideoxyglucosone (3,4-D) derivative	6.56	251.1009
Quinoxaline (Glyoxal (GO) derivative)	7.65	131.0598
Methylquinoxaline (Methylglyoxal (MGO) derivative)	9.40	145.0760
Dimethylquinoxaline (Diacetyl (DA) derivative)	10.82	159.0922
<i>Internal standard</i>		
Quinoxaline-5,6,7,8-d4	7.54	135.0855

Calibration standards at 8 points were prepared in the same diluent as the sample, without o-PDA. The calibration curves were built using the ratio of the chromatogram peak areas (analyte vs internal standard) plotted against the corresponding concentration (0.05 mg.L⁻¹ to 21 mg.L⁻¹ for quinoxaline, 0.01 mg.L⁻¹ to 3 mg.L⁻¹ for methylquinoxaline, and 0.005 mg.L⁻¹ to 1.5 mg.L⁻¹ for dimethylquinoxaline). The calibration curves were linear without forcing the zero-crossing. The calibration curve for quinoxaline was used to quantify several commercially non-available compounds (glucosone, 1-deoxyglucosone, 3-deoxyglucosone and 3,4-dideoxyglucosone derivatives).

The repeatability of the extraction protocol was assessed for 3-deoxyglucosone over eight successive extractions from the same freeze-dried sample, and was found to be excellent (RSD = 0.01%).

2.8 Analysis of furfural and 5-HMF

The extracts prepared for the analysis of glucose and fructose (2.5.1) were stored at -20°C for a maximum of 2 weeks prior to analyzing furfural and 5-HMF.

Furfural and 5-HMF were separated using a Thermo Fisher (Waltham, MA, USA) U3000 System composed of a ternary solvent manager RS pump, a refrigerated RS autosampler at 10°C and a Column compartment oven heated at 40°C, coupled to a photodiode array detector. The stationary phase was an Acquity HSS T3 (100 x 2.1 mm, 1.8 µm) column equipped with a Vanguard precolumn (5 x 2.1 mm) made of the same material. The injection volume was 1.4 µL.

Elution was performed under a 0.5 mL.min⁻¹ flow rate with a combination of two mobile phases: water and acetonitrile (both acidified with 0.1% formic acid) using the following gradient: 95% water for 1.5 min, increased to 100% acetonitrile in 0.1 min, after which the composition was kept for 3.4 min to rinse the system before returning back to 95% water in 0.1 min and finally equilibrating for 6.9 min, the total run duration being 11 min.

Detection was performed at 277 nm and 284 nm for furfural and 5-HMF, respectively.

Calibration with an external standard method was used for quantification. The response range was evaluated for concentrations ranging from 0.05 mg.L⁻¹ to 21.1 mg.L⁻¹ with seven points for both compounds. The calibration curve was linear without forcing the zero-crossing. The *LOD* and *LOQ* values for furfural were equal to 5.93 and 19.8 µg.L⁻¹ respectively, while for 5-HMF they were equal to 0.190 and 0.634 µg.L⁻¹ respectively.

3 Results and Discussion

3.1 Temperature profiles of G and G+L model cakes

Temperatures were measured in the oven and at three specific locations in the cakes during baking: at the interface between the baking pan and the cake (bottom), at the geometric center of the cake (center) and at

the interface between the cake and the air in the oven (surface). The temperature in the oven quickly reached the temperature set-point, contrary to the temperatures inside the cakes which evolved differently during baking (Figure 1, doi.org/10.15454/MI4A3S).

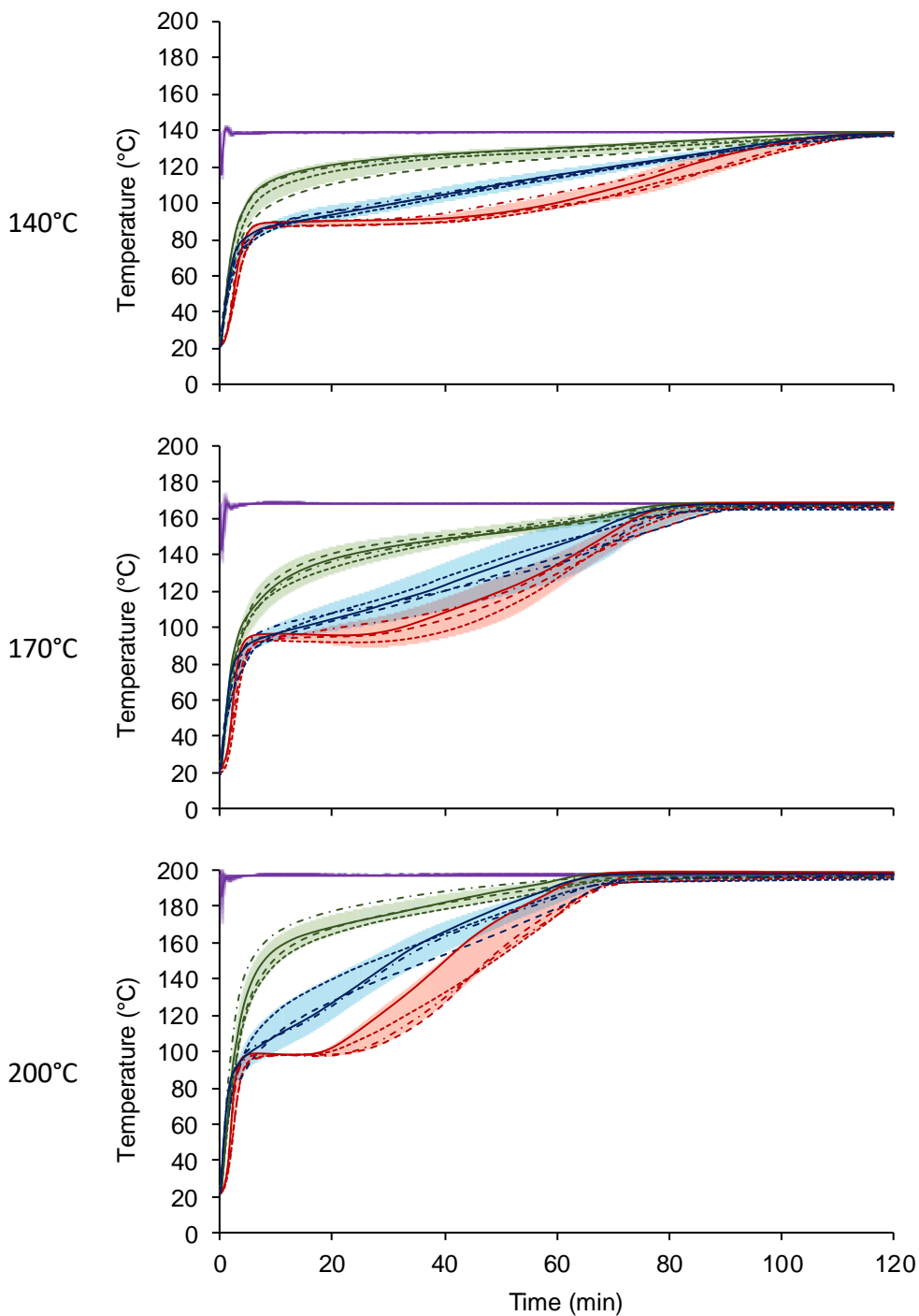


Figure 1. Temperature profile in the oven air (♣) and at the surface (♠), bottom (♣) and center (♠) of the cakes. Colored surfaces represent the standard deviation on either side of the mean, both calculated using all measurements ($n=10$ to 16). Lines represent the mean obtained for each condition: $G-25$ Hz (\cdots), $G+L-25$ Hz ($---$), $G-50$ Hz ($- \cdots -$), $G+L-50$ Hz ($-$) ($n=1$ to 7).

As expected, the surface temperature evolved most rapidly, rising asymptotically towards the oven temperature because it was directly exposed to convection and radiation that promoted water evaporation much more than in the inner layers. The temperature at the center rose the slowest, mainly by conduction through the product which remained wet longer and behaved as a thermal insulator like most food products. Moreover, a plateau was observed whose value and duration varied as a function of the temperature set-point in the oven, corresponding to a balance between the amount of energy supplied by convection and conduction of the air in the oven (convection and radiation on the surface and conduction in the product) and that consumed by water evaporation. The temperature at the bottom remained between these two temperatures. It is worth noting that after a certain baking duration (120 min at 140°C, 90 min at 170°C, 70 min at 200°C), the temperature became uniform in this thin product and equal to that recorded in the oven. The temperature gradients were coupled with mass gradients, so that the concentrations in precursors and newly-formed compounds also varied according to the position in the cakes and over time.

It is important to note that no significant differences between the two formulations and convection levels (fan frequencies) could be detected on the temperature profiles nor on the water content profiles (data not shown, doi.org/10.15454/18HVVK). It can thus be inferred that the reactions induced by the added leucine had no impact on heat and mass transfers in the product. Similarly, a higher level of convection may have caused the surface of the cakes to dry more rapidly, thus generating a faster temperature increase at that point, but no significant changes were found despite the excellent repeatability of the measurements (Figure 1).

3.2 Reaction scheme for glucose and glucose+leucine model cakes

A simplified reaction scheme was established, describing the reactivity of the chosen precursors (glucose or glucose + leucine) added to model cakes prior to baking (Figure 2). The scheme was based on information gathered from the literature and by considering the kinetic evolution of experimentally measured markers (in dotted blue) as well as some key compounds essential to explaining the main reaction pathways (in black). Figure 2 shows that in a caramelization-like system (*G* model cake), glucose can interconvert into either fructose through 1,2-enediol, or glucosone. The conversion to fructose is referred to as 1,2-enolization (Brands & van Boekel, 2001; Martins & van Boekel, 2005), and the isomerization reaction is also known as the Lobry de Bruyn-van Ekenstein rearrangement (Bruyn, 1895). Fructose can also be in equilibrium with 2,3-enediol.

The elimination of water from 1,2-enediol produces 3-deoxyglucosone (3-D), and further water elimination from 3-D leads to the formation of 3,4-dideoxyglucosone (3,4-D) which can then dehydrate to 5-hydroxymethylfurfural (5-HMF) (Perez Locas & Yaylayan, 2008). 1-deoxyglucosone (1-D) is formed by water elimination from 2,3-enediol in the same way as for 3-D, but with an obligatory passage through fructose. It should be noted that in a Maillard-type system (*G+L* model cake), 1-D and 3-D can also form from eneaminals

MGO by retroaldolization chain cleavage (Belitz et al., 2009). However, this second route was not considered in Figure 2 because according to Hollnagel & Kroh, 1998, and Kocadağlı & Gökmen, 2016, it can be assumed that MGO mainly derives from 1-D.

Fructose is assumed to be the source of furfural and 5-HMF (Hu et al., 2018; Kocadağlı & Gökmen, 2016). According to Hu et al. (2018), both furanic compounds were also likely to be formed from 3-D, *via* 3,4-D for 5-HMF. All the intermediates previously mentioned and both furanic compounds were assumed to form brown polymers without leucine (Belitz et al., 2009; Van Boekel, 1998). In the presence of leucine, these intermediates were also assumed to give rise to melanoidins through the Strecker degradation or *via* other reaction pathways (Yaylayan, 2003). Melanoidins differ from the brown polymers previously described in that they contain nitrogen.

3-methylbutanal (3-MB) is the specific Strecker aldehyde for leucine. The best established mechanism for Strecker degradation starts with nucleophilic addition of the amino group of the amino acid to one of the two carbonyl groups of the α -dicarbonyl compound, forming an unstable hemiaminal, which finally decomposes into an α -aminocarbonyl and a Strecker aldehyde (Ho et al., 2015). α -dicarbonyl compounds further undergo polymerization reactions leading to the formation of melanoidins (Bruhns et al., 2019; Kroh et al., 2008; Tressl et al., 2005). Nitrogen-free polymers can be formed by caramelization (Kroh, 1994).

3.3 Effect of precursors and temperature on reaction markers

The contents of all markers were measured kinetically in both model cakes (*G* and *G+L*) at three baking temperatures and two levels of convection. These contents were instantaneous, reflecting an accumulation when the rate of formation reactions was higher than that of consumption reactions. The results in Figure 3 and Figure 4 show the excellent repeatability of the kinetic measurements performed on all baking experiments using the *G* and *G+L* systems.

3.3.1 Consumption of precursors

The consumption of precursors is shown in Figure 3 (doi.org/10.15454/GUXKYQ). The figure shows the rapid consumption of glucose in the *G* model cake during baking at 200°C; this was due to caramelization, with the precursor being almost totally consumed after 90 min of baking. The reaction was clearly less intense at lower set-point temperatures (140°C and 170°C). These results are consistent with the fact that the caramelization requires temperatures above 120°C for glucose degradation (Hurtta et al., 2004; Kroh, 1994). Indeed, for an oven set-point temperature of 200°C, the temperatures measured at the surface and center of the cakes reached 120°C after 5 and 35 min, respectively. These times increased to 8 and 55 min at 170°C and to 20 and 80 min at 140°C (Figure 1).

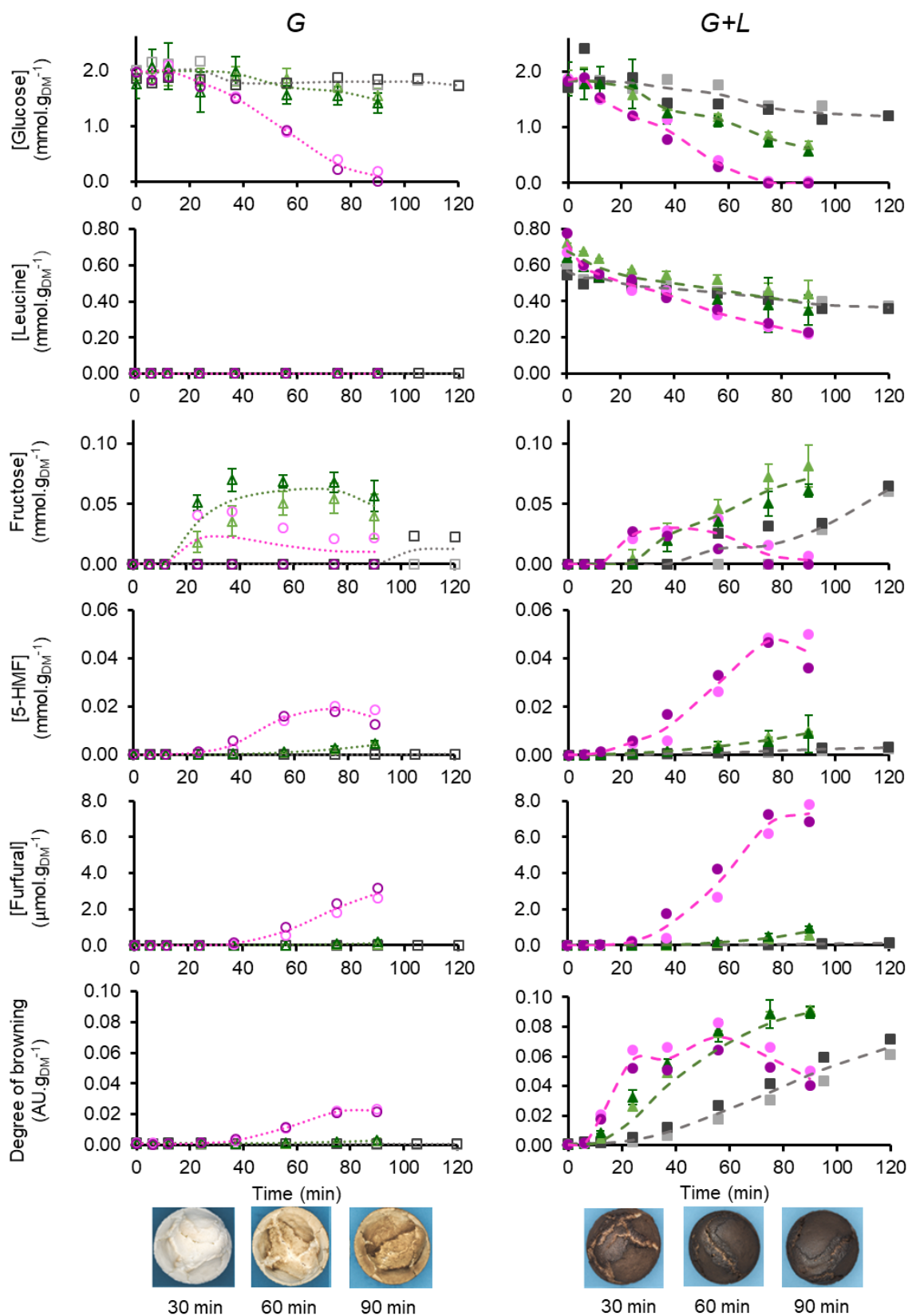


Figure 3. Concentrations of precursors, fructose and furanic compounds and degree of browning at different times during baking of the G (empty symbols) and G+L (full symbols) model cakes at 140°C/25 Hz (\square , \blacksquare , $n=1$), 140°C/50 Hz (\square , \blacksquare , $n=1$), 170°C/25 Hz (\triangle , \blacktriangle , $n=3$), 170°C/50 Hz (\triangle , \blacktriangle , $n=3$), 200°C/25 Hz (\circ , \bullet , $n=1$) and 200°C/50 Hz (\circ , \bullet , $n=1$). Lines show the trend for each temperature considering the two levels of convection as repetitions. The images at the bottom show the browning intensity of G and G+L cakes baked at 200°C for three different baking times.

In the presence of leucine (*G+L* model cake), glucose consumption was higher and more rapid than in *G* model cakes at 140°C and 170°C, because the Maillard reaction was activated at lower temperatures than caramelization. Nevertheless, at 200°C, the glucose consumption rate was quite similar to that measured in the *G* model, with complete consumption in less than 80 min.

The leucine consumption observed thus confirmed activation of the Maillard reaction pathway in the *G+L* model cake at all the baking set-point temperatures tested. The kinetics were very similar at 140°C and 170°C, and consumption was slightly faster at 200°C. However, leucine degradation was significantly lower than that of glucose. This difference may have been due to the fact that the amount of leucine measured was the resultant of the amount of consumed leucine and that regenerated during the Maillard reaction (Figure 2).

3.3.2 Generation and consumption of fructose, a key intermediate

While glucose was consumed, the generation of fructose was most probably detected because of glucose isomerization, as previously shown in Figure 2. With both the *G* and *G+L* formulae, fructose was found during the baking time, with amounts and trends that depended on the oven temperature (Figure 3, doi.org/10.15454/95JTQS). This finding confirms that fructose forms easily from glucose in both the caramelization and Maillard reaction pathways in model cake systems. According to the reaction scheme (Figure 2), fructose can only be formed from glucose (reversibly) and may then be consumed by three or four subsequent reactions (in the *G* and *G+L* models, respectively). The concentrations measured therefore resulted from both the production and degradation of this compound. From a quantitative point of view, fructose accumulation did not exceed 0.08 mmol.g_{DM}⁻¹, for an initial glucose concentration close to 2 mmol.g_{DM}⁻¹. At 140°C, a small quantity of fructose was detected but only at the end of baking in the *G* model cake, while increasing quantities were measured from 56 min in the *G+L* model cake. For both formulae, fructose always displayed higher concentrations at 170°C than at 200°C, which probably meant that fructose consumption became faster than its formation at the higher temperature. Indeed, fructose is known to have a higher reactivity than glucose under low moisture conditions during the Maillard reaction (Jiang et al., 2008; Robert et al., 2004), so a high rate of disappearance could be expected. Moreover, at 170°C, the apparent kinetics of fructose differed markedly between the *G* and *G+L* model cakes. Indeed, with the *G* formula, the fructose that formed was accumulated and then consumed (bell-shaped curve), while at the end of baking in the *G+L* model, its formation was predominant compared to its consumption (curve with a rising trend). This different pattern may have been due to the different fructose consumption pathways activated as a function of the composition of precursors at this temperature.

3.3.3 Furanic and brown products

In both model cakes, the kinetics of 5-HMF and furfural formation were very similar, but 5-HMF was found in much larger quantities than furfural (20 and 50 μmol.g_{DM}⁻¹, in *G* and *G+L*, respectively, for 5-HMF, against

2 and 8 $\mu\text{mol.g}_{\text{DM}}^{-1}$, in *G* and *G+L*, respectively, for furfural, after 80 min at 200°C) (Figure 3, doi.org/10.15454/IICJV3). A short lag phase of approximately 20 min was seen, similar to that seen for fructose, and the effect of temperature was paramount, as reported by Kocadağlı & Gökmen (2016) for the baking of very thin products. The curves in Figure 3 also show that the concentrations of furanic compounds that had formed were markedly increased in the presence of leucine.

Similarly, browning was more pronounced and rapid in the presence of leucine in the *G+L* model cake at all the temperatures tested (Figure 3, doi.org/10.15454/QYCBWIW). Figure 3 shows images of the cakes after the three baking times at 200°C, and the browning levels measured for all kinetics. It can be seen that at 200°C, the measured absorbance decreased at the end of baking, but this was probably due to high molecular weight and water-insoluble melanoidins and brown polymers that were not covered by the measurement.

These results are in line with those obtained by Srivastava et al., 2018 who also showed that browning was specifically localized to the outermost layer of *G* and *G+L* products where local temperatures reached higher values. The difference in browning levels between *G* and *G+L* also indicated a different progression of the reactions and different compositions and characteristics for brown compounds (brown polymers from caramelization or melanoidins from Maillard reaction).

3.3.4 α -dicarbonyl intermediates

Figure 4 (doi.org/10.15454/HV3UTK) shows the quantities of glucosone (GCO), 1-deoxyglucosone (1-D), 3-deoxyglucosone (3-D), 3,4-dideoxyglucosone (3,4-D), methylglyoxal (MGO), and diacetyl (DA) measured during this study. No glyoxal (GO) was detected in the *G* model cake, and very small quantities of GO (between 0.05 and 0.2 $\mu\text{mol.g}_{\text{DM}}^{-1}$) were measured in the *G+L* model and only under the most extreme conditions (200°C, high convection level) (data not shown).

At 140°C, no GCO was measured in the *G* model cake (Figure 4). As it can only be formed by the oxidation of glucose (Jenny & Glomb, 2009), the rate of this reaction must be very slow at 140°C. At 170°C, the GCO concentrations rose gradually up to 0.03 $\mu\text{mol.g}_{\text{DM}}^{-1}$ after 90 min. At 200°C, GCO displayed the bell-shape which peaked at 36 min. In the presence of leucine (*G+L* model cake), the concentrations were much higher than in the *G* model cake with bell-shaped curves for all three temperature levels and a peak was reached more rapidly the higher the set-point temperature. The patterns observed for 1-D were very similar, with faster formation and larger amounts measured. In the *G+L* model, the presence of leucine significantly favored both the formation and consumption of 1-D, and high levels were measured at 140°C. It should be noted that in the case of GCO and 1-D, the experimental curves for both model cakes were the only ones to display a discrepancy between the measurements at 200°C with low or high fan frequencies. This might have been due to a very rapid consumption of these compounds in the crusts of the cakes with a high fan frequency, leading to contents below the LOQ.

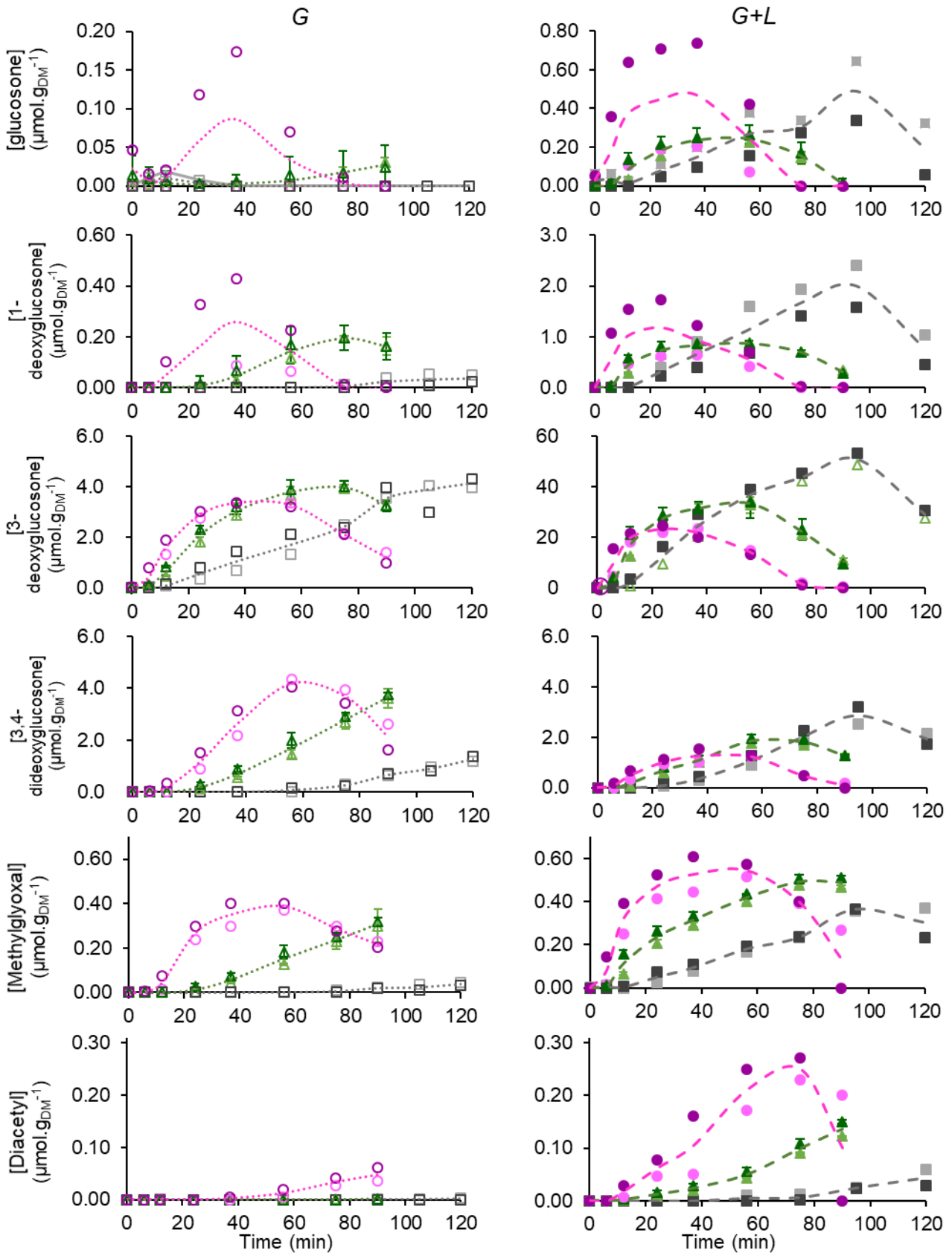


Figure 4. Concentrations of α -dicarbonyl intermediates at different times during baking of the *G* (empty symbols) and *G+L* (full symbols) model cakes at 140°C/25 Hz ($\square, \blacksquare, n=1$), 140°C/50 Hz ($\square, \blacksquare, n=1$), 170°C/25 Hz ($\triangle, \blacktriangle, n=3$), 170°C/50 Hz ($\triangle, \blacktriangle, n=3$), 200°C/25 Hz ($\circ, \bullet, n=1$) and 200°C/50 Hz ($\circ, \bullet, n=1$). Lines indicate the trend for each temperature considering the two levels of convection as repetitions.

3-D was formed in much larger quantities (Figure 4) than GCO (25-fold) and 1-D (10-fold). This was in line with the results obtained by Kocadağlı & Gökmen, 2016, who reported 3-D concentrations that were roughly 26- and 9-fold higher than those of GCO and 1-D, respectively, in a low moisture wheat flour/glucose model system. The shape of the curves was very similar for both the *G* and *G+L* formulae, and an increase in temperature accelerated the formation of 3-D in both cases. However, the amounts in the *G+L* cake were roughly 11-fold higher than in the *G* cake.

The quantities of 3,4-D measured in the *G* model cake were of the same order of magnitude as those of 3-D. 3,4-D formed gradually and more rapidly than it was consumed at 140°C and 170°C, and the reactions were accelerated by temperature (Figure 4). The amount of 3,4-D measured in the *G+L* model was of the same order of magnitude as in the *G* model, but all the kinetics were bell-shaped with a maximum amount that decreased and was reached earlier as the set-point temperature rose.

The formation and degradation kinetics of MGO were very similar in the *G* and *G+L* models (Figure 4), with amounts that were slightly higher in the presence of leucine. Temperature also had an accelerating effect.

In the *G* model cake, only very small amounts of DA could be detected at 200°C under high convection (Figure 4). In the *G+L* model, the formation of DA varied with temperature.

In conclusion, all the kinetics were bell-shaped, typical of the simultaneous formation and degradation of intermediate products and significantly accelerated by temperature. It should be noted that all of these α -dicarbonyl compounds were found in relatively small quantities (in the order of $\mu\text{mol.g}_{\text{DM}}^{-1}$, when the initial concentrations in glucose and leucine were in the order of $\text{mmol.g}_{\text{DM}}^{-1}$). Only GCO, 1-D and 3-D were formed in much larger amounts (about 4 to 10-fold) in the *G+L* model than in the *G* model cake.

3.4 Hypotheses regarding the reaction pathways activated during baking

3.4.1 Glucose degradation pathways

The comparison of the results described in the previous section was designed to highlight the reaction pathways that were activated during the thermal processing of *G* and *G+L* model cakes. Figure 5 shows the markers measured at 170°C and grouped according to the reaction pathways presented in Figure 2. As already mentioned, glucose can be converted into either GCO (one reaction step from glucose), or fructose (two steps) and 3-D (two steps) through 1,2-enediol. Figure 5 shows that a large amount of fructose (Figure 5A) and a relatively smaller quantity of 3-D (Figure 5B) were measured. On the other hand, GCO was only present in a very small quantity (Figure 5C), no glyoxal (GO) was detected and there was no noticeable browning of the cake at that temperature. It can then be inferred that the formation of GCO leading to GO and then to brown polymers was a slow rate reaction, not activated at 170°C in *G* model cake. This suggests that the pathway from glucose to 1,2-enediol and subsequently into fructose and 3-D predominated over the

pathway to GCO. Regarding the reaction kinetics, however, both the amounts and temporalities needed to be taken into account since the reaction rate is dependent on both the reaction rate constant and concentration of substrates. Indeed, a similar trend was observed for fructose and 3-D generation, which started to accumulate after 24 min but with a noticeably higher quantity of fructose (Figure 5A). The initial concentration in glucose being well defined, it could firstly be concluded that the rate constant of glucose degradation to 1,2-enediol was certainly the highest, and secondly that the rate of conversion to fructose was higher than that leading to 3-D. This trend was also confirmed at 200°C.

The time lag in the accumulation of 3,4-D (Figure 5C) and 5-HMF (Figure 5B) compared to that of fructose (Figure 5A) or 3-D (Figure 5B) reflected the fact that their generation required the prior formation of fructose or 3-D. Overall, the kinetic results confirmed the hypothesis advanced in the reaction scheme (Figure 2). 5-HMF required a sufficient quantity of fructose to be formed. As previously stated, fructose (two steps from glucose) accumulated with the same temporality as 3-D (two steps), and gave rise to 5-HMF (three steps) while 3-D was converted into 3,4-D (three steps) which then also formed 5-HMF (four steps in this case). Likewise, 1-D displayed the same time lag as 5-HMF (Figure 5C and B), indicating no accumulation of 2,3-enediol, as otherwise 1-D would have appeared later.

3-D (two steps from glucose) was degraded either directly to 3,4-D (three steps) or to F (three steps) (Figure 2). A clear delay was observed between the kinetics of 3-D and 3,4-D, the latter compound appearing at least 12 min after 3-D (Figure 5B). The accumulation of 3-D enabled the formation of 3,4-D and F according to the reaction scheme, but the quantities of F were much smaller than those of 3,4-D, suggesting that the second reaction was more rapid than the first.

To summarize, 3-D and fructose were formed in one reaction step from 1,2-enediol (Figure 2) and occurred simultaneously (Figure 5B). Likewise, 3,4-D and 5-HMF, which were formed in two reaction steps (Figure 2) from 1,2-enediol, displayed the same temporality (Figure 5B). In other words, the contribution from 3,4-D to 5-HMF probably existed but only made a minor addition to what was formed from fructose.

In theory, F (three steps from glucose) could be formed from fructose as 5-HMF (three steps). But in view of the time lag for its accumulation, this pathway could be set aside in favor of that *via* 3-D (two steps). 1-D (four steps) could also give rise to GO. However, no GO was detected and hardly any DA. This means that the degradation pathway from 1-D to GO and DA could be set aside. MGO appeared simultaneously with 1-D and was even detected in larger quantities than 1-D towards the end of baking. It can thus be assumed that the conversion of 1-D to MGO was certainly very rapid and that the degradation of MGO towards brown pigments was probably slow.

In terms of kinetic modeling in the future, these findings suggest that some pathways probably do not need to be taken into account, such as the formation of F from fructose, or provide indications regarding the relative order of magnitude of certain reaction rates compared to others.

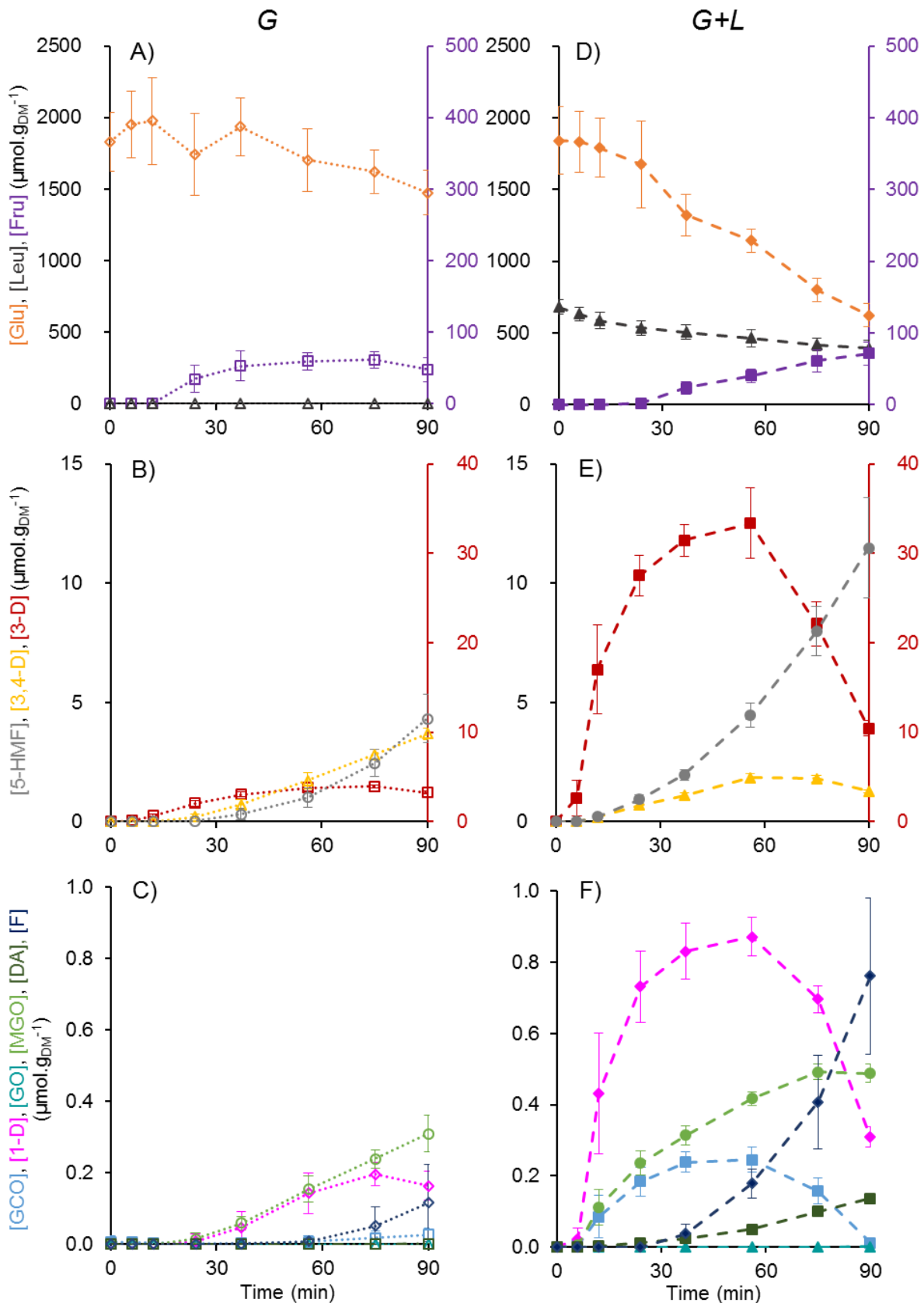


Figure 5. Comparison of concentrations of glucose (Glu, \diamond , \blacklozenge), leucine (Leu, \triangle , \blacktriangle), fructose (Fru, \square , \blacksquare , y-axis on the right), 5-hydroxymethylfurfural (5-HMF, \circ , \bullet), 3,4-dideoxyglucosone (3,4-D, \triangle , \blacktriangle), 3-deoxyglucosone (3-D, \square , \blacksquare , y-axis on the right), glucosone (GCO, \square , \blacksquare), 1-deoxyglucosone (1-D, \diamond , \blacklozenge), glyoxal (GO, \triangle , \blacktriangle), methylglyoxal (MGO, \circ , \bullet), diacetyl (DA, \square , \blacksquare), furfural (F, \diamond , \blacklozenge) during baking of the G (empty symbols, $n=6$) and G+L (full symbols, $n=6$) model cakes at 170°C.

3.4.2 Glucose degradation pathways in the presence of leucine

The rate constants of the reactions described above remain unchanged when leucine is added to the system. Only new reaction pathways that include leucine are supposed to be added. In the presence of leucine (Figure 5), glucose degradation was found to be more important, meaning that the Maillard reaction took precedence over the caramelization of glucose by reaction pathways *via* the eneaminals.

First of all, glucose had three possible degradation pathways in the presence of leucine: 1,2-enediol, GCO and 1,2-eneaminol (Figure 2). More GCO was detected in *G+L* (Figure 5F) due to the activation of 1,2-eneaminol formation, subsequently giving rise to the Amadori product then to GCO. Moreover, a larger quantity of 3-D was detected in *G+L* (Figure 5E) compared to *G* (Figure 5B). This corroborates the activation of 1,2-eneaminol formation that subsequently produced 3-D.

Up to 24 min, the measured quantity of glucose was significantly equivalent with both formulations, *G* (Figure 5A) and *G+L* (Figure 5D). Naturally, the quantity of fructose formed should have been the same because the reaction rate constant and the quantity of substrate were the same. Nevertheless, we measured less fructose in *G+L* up to 56 min (Figure 5D) so that more fructose must have been consumed. If more fructose was consumed, it is necessarily because it moved towards 2,3-eneaminol because the other pathways were identical, as in the case of *G*. This demonstrates how easy it is for reducing sugars to condensate with leucine to form eneaminals. It has often been shown in the literature that the reaction rate constant of eneaminol (or Amadori and Heyns products) is not particularly high but its degradation to deoxyglucosone is relatively high (Carline M. J. Brands & van Boekel, 2003; Kocadağlı & Gökmen, 2016).

Eneaminols undergo leucine-releasing reactions to form the same products as those found in *G* such as GCO, 3-D and 1-D, which were detected in larger quantities in *G+L* (Figure 5E, Figure 5F) than in *G* (Figure 5B, Figure 5C). The quantity of 3-D measured was the result of both the produced and consumed amounts of 3-D. Therefore, if it were higher in *G+L*, then the amount formed was larger because its consumption could not be slowed down, especially because the greater the quantity of 3-D, the more rapid is its degradation. It should be noted that in *G+L*, 3-D could also react with leucine to form 3-MB (Figure 2). The same analogy applies to 1-D and GCO.

The curve of 3,4-D was similar in terms of temporality with both formulations, *G* (Figure 5B) and *G+L* (Figure 5E). 3,4-D appeared earlier and in higher quantities up to 56min (Figure 5E). However, the measured quantity then declined, probably due to the additional degradation pathway towards 3-MB. There was a more pronounced accumulation without leucine, so the pathway giving rise to 5-HMF could be assumed to be slower than that towards 3-MB. Again, the implication is that leucine tended to have an accelerating effect on degradation.

Taken together, these results show that leucine activates new reaction pathways inducing significantly higher concentrations whether starting from glucose or the formed deoxyglucosones.

Since more 1-D was formed in *G+L*, it was natural to detect more DA (Figure 5F), its degradation product. The larger quantity of the substrate gave more product for the same rate constant. The same analogy could be applied to MGO (Figure 5F). GO was not measured in *G+L* (Figure 5F). It is possible that GO was formed from the Amadori product in large quantities, as seen for others, and it may have been degraded towards 3-MB. Nevertheless, the results make it possible to validate the proposed reaction scheme. The dominance of each reaction could be compared and confirmed. Furthermore, identifying reaction markers resulting from α -dicarbonyl intermediates, and kinetic monitoring of them, may enable us to complete the reaction scheme.

4 Conclusions

A simplified reaction scheme has been proposed for the caramelization and Maillard reactions in a product that contains either glucose or glucose with leucine as specific precursors. This reaction scheme made it possible to predict the formation and fate of different markers (precursors, intermediates) that could be quantified in the product as a function of baking conditions (three temperatures, two fan frequencies) and time (from 0 to 90 or 120 min). The simplified reaction scheme, thus established, can describe the reaction pathways of specific precursors (glucose or glucose + leucine) on the basis of information gathered from the literature and enables not only a clearer understanding of the reaction but could also be used for further kinetic modeling.

Working with two identical products that contain either glucose or glucose plus leucine as reactants, it was possible to fully understand the caramelization pattern and the activation of specific pathways by the Maillard reaction. The determination of several intermediate compounds provided some very interesting experimental data to understand and explain the behavior of the precursors. In the context of caramelization, this study showed that the degradation pathway from glucose to 1,2-enediol and subsequently to fructose and 3-D was more important than the pathway to GCO. The formation of GCO and then GO was found to be slow, while the reaction from 2,3-enediol to 1-D was rapid. 5-HMF started to appear when a sufficient quantity of fructose was formed, and 3,4-D only contributed after this step. The formation pathway for furfural *via* 3-D was predominant when compared to that *via* fructose. Moreover, the degradation of MGO towards brown polymers could be supposed to be slow. The formation pathway for GO and DA from 1-D could be set aside as it was negligible. Leucine acts on the Maillard reaction which overrides the caramelization of glucose due to eneaminol reaction pathways. Both glucose and fructose also displayed an ability to react rapidly with leucine.

These data constitute a very complete and original database, that can be very useful for the construction of stoichiokinetic models and quantification of the preponderance of certain reaction pathways to validate the assumptions made in this paper. It will require specific modeling work by coupling transfer equations and chemical reaction models to identify all the reaction constants, taking into account the temperature and water gradients in the products.

Funding

This work was supported by grant from the ABIES doctoral school (Paris-Saclay University).

Acknowledgements

The authors wish to thank Athénaïs Marchand and Joseph-Paul Kenene for images and temperature measurements.

CRedit authorship contribution statement

J. Lee: Conceptualization, Investigation, Methodology, Visualization, Writing – original draft, Writing – review & editing.

S. Roux: Conceptualization, Methodology, Writing – original draft, Writing – review & editing, Supervision.

E. Le Roux: Investigation, Methodology.

S. Keller: Investigation, Methodology.

B. Rega: Conceptualization, Methodology, Writing – original draft, Writing – review & editing, Supervision.

C. Bonazzi: Conceptualization, Methodology, Writing – original draft, Writing – review & editing, Supervision, Project administration, Funding acquisition.

Declaration of Competing Interest

The authors declare that they have no known competing financial

References

Ait Aneur, L., Rega, B., Giampaoli, P., Trystram, G., & Birlouez-Aragon, I. (2008). The fate of furfurals and other volatile markers during the baking process of a model cookie. *Food Chemistry*, *111*(3), 758–763. <https://doi.org/10.1016/j.foodchem.2007.12.062>

Belitz, H.-D., Grosch, W., & Schieberle, P. (2009). *Food chemistry*. Springer-Verlag. <https://doi.org/10.1007/978-3-540-69934-7>

Brands, C. M. J., & van Boekel, M. A. J. . (2001). Reactions of monosaccharides during heating of sugar-casein systems: building of a reaction network model. *J. Agric. Food Chem.*, *49*, 4667.

Brands, C. M. J., & van Boekel, M. A. J. S. (2003). Kinetic modelling of reactions in heated disaccharide–casein systems. *Food Chemistry*, *83*(1), 13–26. [https://doi.org/10.1016/S0308-8146\(03\)00031-1](https://doi.org/10.1016/S0308-8146(03)00031-1)

Bruhns, P., Kanzler, C., Degenhardt, A. G., Koch, T. J., & Kroh, L. W. (2019). Basic Structure of Melanoidins Formed in the Maillard Reaction of 3-Deoxyglucosone and γ -Aminobutyric Acid. *Journal of Agricultural and Food Chemistry*, *67*(18), 5197–5203. https://doi.org/10.1021/ACS.JAFC.9B00202/SUPPL_FILE/JF9B00202_SI_001.PDF

Bruyn, C. A. L. de. (1895). Sur l'hydrate d'hydrazine. *Recueil Des Travaux Chimiques Des Pays-Bas*, *14*(3), 85–

88. <https://doi.org/10.1002/RECL.18950140302>

- Cepeda-Vázquez, M., Rega, B., Descharles, N., & Camel, V. (2018). How ingredients influence furan and aroma generation in sponge cake. *Food Chemistry*, 245, 1025–1033. <https://doi.org/10.1016/J.FOODCHEM.2017.11.069>
- De Vleeschouwer, K., Van der Plancken, I., Van Loey, A., & Hendrickx, M. E. (2009). Modelling acrylamide changes in foods: from single-response empirical to multiresponse mechanistic approaches. *Trends in Food Science & Technology*, 20(3–4), 155–167. <https://doi.org/10.1016/J.TIFS.2009.01.060>
- Fehaili, S., Courel, M., Rega, B., & Giampaoli, P. (2010). An instrumented oven for the monitoring of thermal reactions during the baking of sponge cake. *Journal of Food Engineering*, 101(3), 253–263. <https://doi.org/10.1016/J.JFOODENG.2010.07.003>
- Gökmen, V., Açar, Ö. Ç., Köksel, H., & Acar, J. (2007). Effects of dough formula and baking conditions on acrylamide and hydroxymethylfurfural formation in cookies. *Food Chemistry*, 104(3), 1136–1142. <https://doi.org/http://dx.doi.org/10.1016/j.foodchem.2007.01.008>
- Gökmen, V., Kocadağlı, T., Göncüoğlu, N., & Mogol, B. A. (2012). Model studies on the role of 5-hydroxymethyl-2-furfural in acrylamide formation from asparagine. *Food Chemistry*, 132(1), 168–174. <https://doi.org/10.1016/J.FOODCHEM.2011.10.048>
- Göncüoğlu Taş, N., & Gökmen, V. (2017). Maillard reaction and caramelization during hazelnut roasting: A multiresponse kinetic study. *Food Chemistry*, 221, 1911–1922. <https://doi.org/10.1016/J.FOODCHEM.2016.11.159>
- Hidalgo, F. J., Alaiz, M., & Zamora, R. (1999). Effect of pH and temperature on comparative nonenzymatic browning of proteins produced by oxidized lipids and carbohydrates. *Journal of Agricultural and Food Chemistry*, 47(2), 742–747. <https://doi.org/10.1021/jf980732z>
- Ho, C.-T., Zheng, X., & Li, S. (2015). Tea aroma formation. *Food Science and Human Wellness*, 4(1), 9–27. <https://doi.org/10.1016/J.FSHW.2015.04.001>
- Hodge, J. E. (1953). Dehydrated Foods, Chemistry of Browning Reactions in Model Systems. *Journal of Agricultural and Food Chemistry*, 1(15), 928–943. <https://doi.org/10.1021/jf60015a004>
- Hollnagel, A., & Kroh, L. W. (1998). Formation of α -dicarbonyl fragments from mono- and disaccharides under caramelization and Maillard reaction conditions. *Zeitschrift Für Lebensmitteluntersuchung Und -Forschung A*, 207(1), 50–54. <https://doi.org/10.1007/s002170050294>
- Hu, B., Lu, Q., Jiang, X., Dong, X., Cui, M., Dong, C., & Yang, Y. (2018). Pyrolysis mechanism of glucose and mannose: The formation of 5-hydroxymethyl furfural and furfural. *Journal of Energy Chemistry*, 27(2), 486–501. <https://doi.org/10.1016/J.JECHEM.2017.11.013>
- Hurtta, M., Pitka, I., & Knuutinen, J. (2004). Melting behaviour of D-sucrose, D-glucose and D-fructose. *Carbohydrate Research*, 339(13), 2267–2273. <https://doi.org/10.1016/j.carres.2004.06.022>
- Jenny, G., & Glomb, M. A. (2009). Degradation of glucose: reinvestigation of reactive α -dicarbonyl

- compounds. *Journal of Agricultural and Food Chemistry*, 57(18), 8591–8597. <https://doi.org/10.1021/jf9019085>
- Jiang, B., Liu, Y., Bhandari, B., & Zhou, W. (2008). Impact of Caramelization on the Glass Transition Temperature of Several Caramelized Sugars. Part I: Chemical Analyses. *Journal of Agricultural and Food Chemistry*, 56(13), 5138–5147. <https://doi.org/10.1021/jf703791e>
- Jusino, M. G., Ho, C. T., & Tong, C. H. (1997). Formation Kinetics of 2,5-Dimethylpyrazine and 2-Methylpyrazine in a Solid Model System Consisting of Amioca Starch, Lysine, and Glucose. *Journal of Agricultural and Food Chemistry*, 45(8), 3164–3170. <https://doi.org/10.1021/jf960819p>
- Kocadağlı, T., & Gökmen, V. (2016). Multiresponse kinetic modelling of Maillard reaction and caramelisation in a heated glucose/wheat flour system. *Food Chemistry*, 211, 892–902. <https://doi.org/10.1016/j.foodchem.2016.05.150>
- Kroh, L. W. (1994). Caramelisation in food and beverages. *Food Chemistry*, 51(4), 373–379. [https://doi.org/10.1016/0308-8146\(94\)90188-0](https://doi.org/10.1016/0308-8146(94)90188-0)
- Kroh, L. W., Fiedler, T., & Wagner, J. (2008). α -Dicarbonyl Compounds—Key Intermediates for the Formation of Carbohydrate-based Melanoidins. *Annals of the New York Academy of Sciences*, 1126(1), 210–215. <https://doi.org/10.1196/ANNALS.1433.058>
- Lee, J., Bousquières, J., Descharles, N., Roux, S., Michon, C., Rega, B., & Bonazzi, C. (2020). Potential of model cakes to study reaction kinetics through the dynamic on-line extraction of volatile markers and TD-GC-MS analysis. *Food Research International*, 132, 109087. <https://doi.org/10.1016/j.foodres.2020.109087>
- Martins, S. I. F. S., Jongen, W. M. F., & van Boekel, M. A. J. S. (2000). A review of Maillard reaction in food and implications to kinetic modelling. *Trends in Food Science & Technology*, 11(9–10), 364–373. [https://doi.org/10.1016/S0924-2244\(01\)00022-X](https://doi.org/10.1016/S0924-2244(01)00022-X)
- Martins, S. I. F. S., & van Boekel, M. A. J. S. (2003). Kinetic modelling of Amadori N-(1-deoxy-d-fructos-1-yl)-glycine degradation pathways. Part II—Kinetic analysis. *Carbohydrate Research*, 338(16), 1665–1678. [https://doi.org/10.1016/S0008-6215\(03\)00174-5](https://doi.org/10.1016/S0008-6215(03)00174-5)
- Martins, S. I. F. S., & van Boekel, M. A. J. S. (2005). A kinetic model for the glucose/glycine Maillard reaction pathways. *Food Chemistry*, 90(1), 257–269. <https://doi.org/10.1016/j.foodchem.2004.04.006>
- Nguyen, H. T., Van der Fels-Klerx, H. J. (Ine), Peters, R. J. B., & Van Boekel, M. A. J. S. (2016). Acrylamide and 5-hydroxymethylfurfural formation during baking of biscuits: Part I: Effects of sugar type. *Food Chemistry*, 192, 575–585. <https://doi.org/10.1016/j.foodchem.2015.07.016>
- Nursten, H. (2005). *The Maillard Reaction: Chemistry, Biochemistry and Implications*. Royal Society of Chemistry. <https://doi.org/10.1039/9781847552570>
- Perez Locas, C., & Yaylayan, V. A. (2008). Isotope Labeling Studies on the Formation of 5-(Hydroxymethyl)-2-furfuraldehyde (HMF) from Sucrose by Pyrolysis-GC/MS. *Journal of Agricultural and Food Chemistry*, 56(15), 6717–6723. <https://doi.org/10.1021/jf8010245>

- Rainer Cremer, D., & Eichner, K. (2000). The reaction kinetics for the formation of Strecker aldehydes in low moisture model systems and in plant powders. *Food Chemistry*, 71(1), 37–43. [https://doi.org/10.1016/S0308-8146\(00\)00122-9](https://doi.org/10.1016/S0308-8146(00)00122-9)
- Robert, F., Vuataz, G., Pollien, P., Saucy, F., Alonso, M. I., Bauwens, I., & Blank, I. (2004). Acrylamide formation from asparagine under low-moisture Maillard reaction conditions. 1. Physical and chemical aspects in crystalline model systems. *Journal of Agricultural and Food Chemistry*, 52(22), 6837–6842. <https://doi.org/10.1021/jf0492464>
- Shibamoto, T. (2014). Diacetyl: Occurrence, analysis, and toxicity. *Journal of Agricultural and Food Chemistry*, 62(18), 4048–4053. <https://doi.org/10.1021/jf500615u>
- Srivastava, R., Bousquières, J., Cepeda-Vázquez, M., Roux, S., Bonazzi, C., & Rega, B. (2018). Kinetic study of furan and furfural generation during baking of cake models. *Food Chemistry*, 267, 329–336. <https://doi.org/10.1016/j.foodchem.2017.06.126>
- Tressl, R., Kersten, E., Wondrak, G., Rewicki, D., & Krüger, R.-P. (2005). Fragmentation of Sugar Skeletons and Formation of Maillard Polymers. *The Maillard Reaction in Foods and Medicine*, 69–75. <https://doi.org/10.1533/9781845698447.2.69>
- Van Boekel, M. A. J. S. (1998). Effect of heating on Maillard reactions in milk. *Food Chemistry*, 62(4), 403–414. [https://doi.org/10.1016/S0308-8146\(98\)00075-2](https://doi.org/10.1016/S0308-8146(98)00075-2)
- Velíšek, J. (2014). *The chemistry of food*. John Wiley & Sons, Ltd.
- Yaylayan, V. A. (2003). Recent Advances in the Chemistry of Strecker Degradation and Amadori Rearrangement: Implications to Aroma and Color Formation. *Food Sci. Technol. Res*, 9(1), 1–6.
- Yaylayan, V. A., & Keyhani, A. (2000). Origin of carbohydrate degradation products in L-alanine/D-[13C]glucose model systems. *Journal of Agricultural and Food Chemistry*, 48(6), 2415–2419. <https://doi.org/10.1021/jf000004n>
- Zehentbauer, G., & Grosch, W. (1998). Crust Aroma of Baguettes I. Key Odorants of Baguettes Prepared in Two Different Ways. *Journal of Cereal Science*, 28(1), 81–92. <https://doi.org/10.1006/JCRS.1998.0184>